Numerical Modeling of Coupled Thermoelasticity with relaxation times in Rotating FGAPs Subjected to a Moving Heat Source

Abstract. The time-stepping DRBEM modeling was proposed to study the 2D dynamic response of functionally graded anisotropic plate (FGAP) subjected to a moving heat source. The FGAP is assumed to be graded through the thickness. The main aim of this paper is to evaluate the difference between Green and Lindsay (G-L) and Lord and Shulman (L-S) theories of coupled thermo-elasticity in rotating FGAP subjected to a moving heat source. The accuracy of the proposed method was examined and confirmed by comparing the obtained results with those known previously.
.

Keywords: Thermoelasticity; Functionally Graded Anisotropic Plates; Boundary Element Method.

1. Introduction

Biot [1] introduced the classical coupled theory of thermoelasticity (CCTE) to overcome the paradox inherent in the classical uncoupled theory that elastic changes have no effect on temperature. The heat equations for both theories are a diffusion type predicting infinite speeds of propagation for heat waves contrary to physical observations. Most of the approaches that came out to overcome the unacceptable prediction of the classical theory are based on the general notion of relaxing the heat flux in the classical Fourier heat conduction equation, thereby introducing a non-Fourier effect. A flux rate term into Fourier law of heat conduction is incorporated by Lord and Shulman (L-S) [2], who formulated an extended thermoelasticity theory (ETE) which is also known as the theory of generalized thermoelasticity with one relaxation time and the Fourier's heat conduction equation is modified. Another thermoelasticity theory that admits the second sound effect is reported by Green and Lindsay (G-L) [3], who developed a temperature-rate-dependent thermoelasticity theory (TRDTE) which is also called the theory of generalized thermoelasticity with two relaxation times by introducing two relaxation times that relate the stress and entropy to the temperature.

Functionally graded Plates (FGPs) are a type of nonhomogeneous composites usually made from a mixture of metals and ceramics. FGPs are now developed for general use as structure components in ultrahigh temperature environments and extremely large thermal gradients such as aircraft, space vehicles, automobile industries, nuclear plants, and other engineering applications. For a functionally graded plate (FGP) the material properties are generally assumed to vary continuously in the thickness direction only. The response of an FGP to mechanical and thermal loads may be computed analytically, numerically, or experimentally. We are not aware of experimental results on FGPs subjected to transient thermal, magnetic, and mechanical loads. It is well known that the thermal stress distributions in a transient state can show large values compared with the one in a steady state. Therefore, the transient thermoelastic problems for these nonhomogeneous materials become important, and there are several studies concerned with these problems, such as Skouras et al. [4], Mojdehi et al. [5], Zhou et al. [6], Loghman et al. [7], Sun and Luo [8] and Mirzaei and Dehghan [9] are examples involving functionally graded materials.

In recent years, the dynamical problem of thermo-elasticity for functionally graded anisotropic plates (FGAPs) becomes more important due to its many applications in modern aeronautics, astronautics, earthquake engineering, soil dynamics, mining engineering, plasma physics, nuclear reactors and high-energy particle accelerators, for instance. Abd-Alla [10] obtained the relaxation effects on reflection of generalized magneto-thermo-elastic waves. Abd-Alla and Al-Dawy [11] obtained the relaxation effects on Rayleigh waves in generalized thermoelastic media. Abbas and Abd-Alla [12, 13] studied generalized thermoelastic problems for an infinite fibre-reinforced anisotropic plate. Xia, et al. [14] used a time domain finite element method to solve dynamic response of two-dimensional generalized thermoelastic coupling problem subjected to a moving heat source based on Lord and Shulman theory with one thermal relaxation time

It is hard to find the analytical solution of a problem in a general case, therefore, an important number of engineering and mathematical papers devoted to the numerical solution have studied the overall behavior of such materials (see, e.g., El-Naggar et al. [15, 16], Abd-Alla et al. [17-19], Qin [20], Sladek et al. [21], Tian et al. [22], Fahmy [23-28], Fahmy and El-Shahat [29], Othman and Song, [30], Davi and Milazzo [31], Hou et al. [32], [Abreu et al. [33], Espinosa and Mediavilla, [34].

One of the most frequently used techniques for converting the domain integral into a boundary one is the so-called dual reciprocity boundary element method (DRBEM). This method was initially developed by Nardini and Brebbia [35] in the context of two-dimensional (2D) elastodynamics and has been extended to deal with a variety of problems wherein the domain integral may account for linear-nonlinear static-dynamic effects. A more extensive historical review and applications of dual reciprocity boundary element method may be found in [Brebbia et al. [36], Wrobel and Brebbia [37], Partridge and Brebbia [38], Partridge and Wrobel [39] and Fahmy [40-47]].

The main objective of this paper is to study the model of two-dimensional equations of coupled thermo-elasticity with one and two relaxation times in rotating FGAPs subjected to a moving heat source. A predictor-corrector implicit-explicit time integration algorithm was developed and implemented for use with the dual reciprocity boundary element method (DRBEM) to obtain the solution for the temperature and displacement fields. The accuracy of the proposed method was examined and confirmed by comparing the obtained results with those known before.

.

2. Formulation of the problem

Consider a Cartesian coordinates system 0xyz as shown in Fig. 1. We shall consider a functionally graded anisotropic plate rotating about it with a constant angular velocity. The plate occupies the region $R = \left\{(x, y, z): 0 < x < \underline{\gamma}, 0 < y < \underline{\beta}, 0 < z < \underline{\alpha}\right\}$ with graded material properties in the thickness direction.

In this chapter, the material is functionally graded along the 0x direction. Thus, the governing equations of generalized thermo-elasticity in the context of the Green and Lindsay theory can be written in the following form:

$$\sigma_{ab,b} - \rho(x+1)^m \omega^2 x_a = \rho(x+1)^m \ddot{u}_a, \tag{1}$$

$$\sigma_{ab} = (x+1)^m \left[C_{abfg} u_{f,g} - \beta_{ab}\left(T - T_0 + \tau_1 \dot{T}\right)\right], \tag{2}$$

$$k_{ab} T_{,ab} = \beta_{ab} T_0 \dot{u}_{a,b} + \rho c (x+1)^m \left[\dot{T} + \tau_2 \ddot{T}\right]. \tag{3}$$

where σ_{ab} is the mechanical stress tensor, u_k is the displacement, T is the temperature, C_{abfg} and β_{ab} are respectively, the constant elastic moduli and stress-temperature coefficients of the anisotropic medium, ω is the uniform angular velocity, k_{ab} are the thermal conductivity coefficients satisfying the symmetry relation $k_{ab} = k_{ba}$ and the strict inequality $(k_{12})^2 - k_{11}k_{22} < 0$ holds at all points in the medium, ρ is the density, c is the specific heat capacity, τ is the time, τ_1 and τ_2 are mechanical relaxation times.

3. Numerical implementation

Making use of (2), we can write (1) as follows

$$L_{gb}u_f = \rho\ddot{u}_a - \left(D_a T + \Lambda D_{a1f}u_f - \rho\omega^2 x_a\right) = f_{gb}, \tag{4}$$

where

$$L_{gb} = D_{abf}\frac{\partial}{\partial x_b}, D_{abf} = C_{abfg}\varepsilon, \varepsilon = \frac{\partial}{\partial x_g}, \Lambda = \frac{m}{x+1},$$

$$D_a = -\beta_{ab}\left(\frac{\partial}{\partial x_b} + \delta_{b1}\Lambda + \tau_1\left(\frac{\partial}{\partial x_b} + \Lambda\right)\frac{\partial}{\partial \tau}\right), f_{gb} = \rho\ddot{u}_a - \left(D_a T + \Lambda D_{a1f}u_f - \rho\omega^2 x_a\right).$$

The field equations can now be written in operator form as follows

$$L_{gb}u_f = f_{gb}, \tag{5}$$

$$L_{ab}T = f_{ab}, \tag{6}$$

where the operators L_{gb} and f_{gb} are defined in equation (4), and the operators L_{ab} and f_{ab} are defined as follows

$$L_{ab} = k_{ab}\frac{\partial}{\partial x_a}\frac{\partial}{\partial x_b}, \tag{7}$$

$$f_{ab} = \rho c(x+1)^m\left[\dot{T} + \tau_2\ddot{T}\right] + \beta_{ab}T_0\dot{u}_{a,b}. \tag{8}$$

Using the weighted residual method (WRM), the differential equation (5) is transformed into an integral equation

$$\int_R \left(L_{gb}u_f - f_{gb}\right)u_{da}^*\,dR = 0. \tag{9}$$

Now, we choose the fundamental solution u_{df}^* as weighting function as follows

$$L_{gb}u_{df}^* = -\delta_{ad}\delta(x,\xi). \tag{10}$$

The corresponding traction field can be written as

$$t_{da}^* = C_{abfg}u_{df,g}^* n_b. \tag{11}$$

The thermo-elastic traction vector can be written as follows

$$t_a = \frac{\bar{t}_a}{(x+1)^m} = \left(C_{abfg}u_{f,g} - \beta_{ab}\left(T - T_0 + \tau_1\dot{T}\right)\right)n_b. \tag{12}$$

Applying integration by parts to (9) using the sifting property of the Dirac distribution, with (10) and (12), we can write the following elastic integral representation formula

$$u_d(\xi) = \int_C (u_{da}^* t_a - t_{da}^* u_a + u_{da}^*\beta_{ab}Tn_b)\,dC - \int_R f_{gb}u_{da}^* dR. \tag{13}$$

The fundamental solution T^* of the thermal operator L_{ab}, defined by

$$L_{ab}T^* = -\delta(x,\xi). \tag{14}$$

By implementing the WRM and integration by parts, the differential equation (6) is transformed into the thermal reciprocity equation

$$\int_R (L_{ab}TT^* - L_{ab}T^*T)dR = \int_C (q^*T - qT^*)dC, \tag{15}$$

Where the heat fluxes are independent of the elastic field and can be expressed as follows:

$$q = -k_{ab}T_{,b}n_a, \tag{16}$$

$$q^* = -k_{ab}T_{,b}^*n_a. \tag{17}$$

By the use of sifting property, we obtain from (16) the thermal integral representation formula

$$T(\xi) = \int_C (q^* T - q T^*) dC - \int_R f_{ab} T^* dR. \tag{18}$$

The integral representation formulae of elastic and thermal fields (13) and (18) can be combined to form a single equation as follows

$$\begin{bmatrix} u_d(\xi) \\ T(\xi) \end{bmatrix} = \int_C \left\{ - \begin{bmatrix} t_{da}^* & -u_{da}^* \beta_{ab} n_b \\ 0 & -q^* \end{bmatrix} \begin{bmatrix} u_a \\ T \end{bmatrix} + \begin{bmatrix} u_{da}^* & 0 \\ 0 & -T^* \end{bmatrix} \begin{bmatrix} t_a \\ q \end{bmatrix} \right\} dC$$

$$- \int_R \begin{bmatrix} u_{da}^* & 0 \\ 0 & -T^* \end{bmatrix} \begin{bmatrix} f_{gb} \\ -f_{ab} \end{bmatrix} dR. \tag{19}$$

It is convenient to use the contracted notation to introduce generalized thermo elastic vectors and tensors, which contain corresponding elastic and thermal variables as follows:

$$U_A = \begin{cases} u_a & a = A = 1,2,3; \\ T & A = 4, \end{cases} \tag{20}$$

$$T_A = \begin{cases} t_a & a = A = 1,2,3; \\ q & A = 4, \end{cases} \tag{21}$$

$$U_{DA}^* = \begin{cases} u_{da}^* & d = D = 1,2,3; a = A = 1,2,3; \\ 0 & d = D = 1,2,3; A = 4; \\ 0 & D = 4; a = A = 1,2,3; \\ -T^* & D = 4; A = 4, \end{cases} \tag{22}$$

$$\tilde{T}_{DA}^* = \begin{cases} t_{da}^* & d = D = 1,2,3; a = A = 1,2,3; \\ -\tilde{u}_d^* & d = D = 1,2,3; A = 4; \\ 0 & D = 4; a = A = 1,2,3; \\ -q^* & D = 4; A = 4, \end{cases} \tag{23}$$

$$\tilde{u}_d^* = u_{da}^* \beta_{af} n_f. \tag{24}$$

The thermo-elastic representation formula (19) can be written in contracted notation as:

$$U_D(\xi) = \int_C \left(U_{DA}^* T_A - \tilde{T}_{DA} U_A \right) dC - \int_R U_{DA}^* S_A dR, \tag{25}$$

The vector S_A can be written in the split form as follows

$$S_A = S_A^0 + S_A^T + S_A^u + S_A^{\dot{T}} + S_A^{\ddot{T}} + S_A^{\dot{u}} + S_A^{\ddot{u}}, \tag{26}$$

where

$$S_A^0 = \begin{cases} \rho \omega^2 x_a & a = A = 1,2,3; \\ 0 & A = 4, \end{cases} \tag{27}$$

$$S_A^T = \omega_{AF} U_F \quad with \quad \omega_{AF} = \begin{cases} -D_a & A = 1,2,3; F = 4; \\ 0 & otherwise, \end{cases} \tag{28}$$

$$S_A^u = -\left(D_{af} + \Lambda D_{a1f} \right) \mho U_F$$

With $\mho = \begin{cases} 1 & a = A = 1,2,3; f = F = 1,2,3; \\ 0 & otherwise, \end{cases}$ (29)

$$S_A^{\dot{T}} = -\rho c (x+1)^m \delta_{AF} \dot{U}_F \ with \ \delta_{AF} = \begin{cases} 1 & A = 4; F = 4; \\ 0 & otherwise, \end{cases} \tag{30}$$

$$S_A^{\ddot{T}} = -\rho c (x+1)^m \tau_2 \delta_{AF} \ddot{U}_F, \tag{31}$$

$$S_A^{\dot{u}} = -T_0 Å \delta_{1j} \beta_{fg} \varepsilon \dot{U}_F, \tag{32}$$

$$S_A^{\ddot{u}} = \ddot{U}_F \quad with = \begin{cases} \rho & A = 1,2,3;\ F = 1,2,3; \\ 0 & A = 4;\ f = F = 4. \end{cases} \tag{33}$$

The thermo-elastic representation formula (19) can also be written in matrix form as follows:

$$[S_A] = \begin{bmatrix} \rho\omega^2 x_a \\ 0 \end{bmatrix} + \begin{bmatrix} -D_a T \\ 0 \end{bmatrix} + \begin{bmatrix} -\left(D_{af} + \Lambda D_{a1f}\right)u_f \\ 0 \end{bmatrix}$$
$$+ \left(\rho c (x+1)^m\right) \begin{bmatrix} 0 \\ \dot{T} \end{bmatrix} - \rho c (x+1)^m \tau_2 \begin{bmatrix} 0 \\ \ddot{T} \end{bmatrix} - T_0 \begin{bmatrix} 0 \\ \beta_{ab}\dot{u}_{a,b} \end{bmatrix} + \begin{bmatrix} \rho \ddot{u}_a \\ 0 \end{bmatrix}. \tag{34}$$

Our task now is to implement the DRBEM. To transform the domain integral in (25) to the boundary, we approximate the source vector S_A in the domain as usual by a series of given tensor functions f_{AN}^q and unknown coefficients α_N^q

$$S_A \approx \sum_{q=1}^{N} f_{AN}^q \alpha_N^q. \tag{35}$$

According to the DRBEM, the surface of the solid has to be discretized into boundary elements. In order to make the implementation easy to compute, we use N_b collocation points on the boundary C and another N_i in the interior of R so that the total number of interpolation points is $N = N_b + N_i$.

Thus, the thermo-elastic representation formula (25) can be written in the following form

$$U_D(\xi) = \int_C \left(U_{DA}^* T_A - \tilde{T}_{DA}^* U_A\right) dC - \sum_{q=1}^{N} \int_R U_{DA}^* f_{AN}^q dR\, \alpha_N^q. \tag{36}$$

By applying the WRM to the following inhomogeneous elastic and thermal equations:

$$L_{gb} u_{fn}^q = f_{an}^q, \tag{37}$$

$$L_{ab} T^q = f_{pj}^q, \tag{38}$$

where the weighting functions are chosen to be the elastic and thermal fundamental solutions u_{da}^* and T^*. Then the elastic and thermal representation formulae are similar to those of Fahmy [42] within the context of the uncoupled theory and are given as follows

$$u_{de}^q(\xi) = \int_C \left(u_{da}^* t_{ae}^q - t_{da}^* u_{ae}^q\right) dC - \int_R u_{da}^* f_{ae}^q dR, \tag{39}$$

$$T^q(\xi) = \int_C \left(q^* T^q - q^q T^*\right) dC - \int_R f^q T^* dR. \tag{40}$$

The dual representation formulae of elastic and thermal fields can be combined to form a single equation as follows

$$U_{DN}^q(\xi) = \int_C \left(U_{DA}^* T_{AN}^q - T_{DA}^* U_{AN}^q\right) dC - \int_R U_{DA}^* f_{AN}^q dR, \tag{41}$$

With the substitution of (41) into (36), the dual reciprocity representation formula of coupled thermo elasticity can be expressed as follows

$$U_D(\xi) = \int_C \left(U_{DA}^* T_A - \tilde{T}_{DA}^* U_A\right) dC + \sum_{q=1}^{N} \left(U_{DN}^q(\xi) + \int_C \left(T_{DA}^* U_{AN}^q - U_{DA}^* T_{AN}^q\right) dC \right) \alpha_N^q. \tag{42}$$

To calculate interior stresses, (42) is differentiated with respect to ξ_l as follows

$$\frac{\partial U_D(\xi)}{\partial \xi_l} = -\int_C \left(U^*_{DA,l} T_A - \check{T}^*_{DA,l} U_A\right) dC + \sum_{q=1}^{N} \left(\frac{\partial U^q_{DN}(\xi)}{\partial \xi_l} - \int_C \left(T^*_{DA,l} U^q_{AN} - U^*_{DA,l} T^q_{AN}\right) dC \right) \alpha^q_N. \tag{43}$$

According to the steps described in Fahmy [43], the dual reciprocity boundary integral equation (42) can be written in the following system of equations

$$\tilde{\check{\zeta}} \breve{u} - \eta \check{t} = \left(\zeta \breve{U} - \eta \check{\wp}\right) \alpha. \tag{44}$$

It is important to note the difference between the matrices ζ and $\check{\zeta}$: whereas ζ contains the fundamental solution T^*_M, the matrix $\check{\zeta}$ contains the modified fundamental tensor $\check{T}^*_M$ with the coupling term.

The technique was proposed by Partridge et al. [48] can be extended to treat the convective terms, then the generalized displacements U_F and velocities $\dot{U}_F$ are approximated by a series of tensor functions f^q_{FD} and unknown coefficients γ^q_D and $\tilde{\gamma}^q_D$

$$U_F \approx \sum_{q=1}^{N} f^q_{FD}(x) \gamma^q_D, \tag{45}$$

$$\dot{U}_F \approx \textstyle\sum_{q=1}^{N} f^q_{FD}(x) \tilde{\gamma}^q_D, \tag{46}$$

The gradients of the generalized displacement and velocity can be approximated as follows

$$U_{F,g} \approx \sum_{q=1}^{N} f^q_{K,g}(x) \gamma^q_K, \tag{47}$$

$$\dot{U}_{F,g} \approx \sum_{q=1}^{N} f^q_{FD,g}(x) \tilde{\gamma}^q_D. \tag{48}$$

These approximations are substituted into equations (28) and (32) to approximate the corresponding source terms as follows

$$S^T_A = \sum_{q=1}^{N} S^{T,q}_{AD} \gamma^q_D, \tag{49}$$

$$S^{\dot{u}}_A = -T_0 \beta_{fg} \varepsilon \sum_{q=1}^{N} S^{\dot{u},q}_{AD} \tilde{\gamma}^q_D, \tag{50}$$

where

$$S^{T,q}_{AD} = S_{AF} f^q_{FD,g}, \tag{51}$$

$$S^{\dot{u},q}_{AD} = S_{FA} f^q_{FD,g}. \tag{52}$$

The same point collocation procedure described in Gaul, et al. [49] can be applied to (35), (45) and (46). This leads to the following system of equations

$$\check{S} = J\alpha, \qquad U = J'\gamma, \qquad \dot{U} = J'\tilde{\gamma}. \tag{53}$$

Similarly, the application of the point collocation procedure to the source terms equations (29), (30), (31), (33), (49) and (50) leads to the following system of equations

$$\check{S}^u = -\left(D_{af} + \Lambda D_{a1f}\right) \mho U_F \qquad \textit{With}$$

$$\mho = \begin{cases} 1 & a = A = 1,2,3;\ f = F = 1,2,3; \\ 0 & otherwise, \end{cases} \tag{54}$$

$$\check{S}^{\dot{T}} = \rho c (x+1)^m \delta_{AF} \dot{U}, \tag{55}$$

$$\check{S}^{\ddot{T}} = -c\rho(x+1)^m \tau_2 \delta_{AF} \ddot{U}, \tag{56}$$
$$\check{S}^{\ddot{u}} = \tilde{A}\ddot{U}, \tag{57}$$
$$\check{S}^{T} = \mathcal{B}^T \gamma, \tag{58}$$
$$\check{S}^{\dot{u}} = -T_0 \beta_{fg} \varepsilon \mathcal{B}^{\dot{u}} \tilde{\gamma}. \tag{59}$$

Solving the system (53) forα, γ and $\tilde{\gamma}$ yields

$$\alpha = J^{-1}\check{S}, \qquad \gamma = J'^{-1}U, \qquad \tilde{\gamma} = J'^{-1}\dot{U}, \tag{60}$$

Now, the coefficients α can be expressed in terms of nodal values of the unknown displacements U, velocities $\breve{\dot{U}}$ and accelerations $\breve{\ddot{U}}$ as follows:

$$\alpha = J^{-1}\Big(\check{S}^0 + \big[\mathcal{B}^T J'^{-1} - \big(D_{af} + \Lambda D_{a1f}\big)\mho\big]U + \big[\rho c(x+1)^m \delta_{AF} - T_0 \beta_{fg} \varepsilon \mathcal{B}^{\dot{u}} J'^{-1}\big]\dot{U} \\ + \big[\tilde{A} - \rho c(x+1)^m \tau_2 \delta_{AF}\big]\ddot{U}\Big), \tag{61}$$

Where $\widetilde{A}$ and $\mathcal{B}^T$ are assembled using the sub matrices [ ] and ω_{AF} respectively.

Substituting from Eq. (61) into Eq. (44), we obtain

$$M\ddot{U} + \Gamma\dot{U} + KU = \mathbb{Q}, \tag{62}$$

In which M, Γ, K and $\mathbb{Q}$ are independent of time and are defined by

$$V = \big(\eta\breve{\wp} - \zeta\breve{U}\big)J^{-1}, \qquad M = V\big[\tilde{A} - c\rho(x+1)^m \tau_2 \delta_{AF}\big],$$
$$\Gamma = V\big[\rho c(x+1)^m \delta_{AF} - T_0 \beta_{fg} \varepsilon \mathcal{B}^{\dot{u}} J'^{-1}\big],$$
$$K = \tilde{\zeta} + V\big[\mathcal{B}^T J'^{-1} + \big(D_{af} + \Lambda D_{a1f}\big)\mho\big], \quad \mathbb{Q} = \eta T + V\check{S}^0, \tag{63}$$

Where V, M, Γ and K represent the volume, mass, damping and stiffness matrices, respectively; $\ddot{U}, \dot{U}, U$ and $\mathbb{Q}$ represent the acceleration, velocity, displacement and external force vectors, respectively. The initial value problem consists of finding the function $U = U(\tau)$ satisfying equation (62) and the initial conditions $U(0) = U_0$, $\dot{U}(0) = V_0$ where U_0, V_0 are given vectors of initial data. Then, from Eq. (62), we can compute the initial acceleration vector W_0 as follows

$$MW_0 = \mathbb{Q}_0 - \Gamma V_0 - KU_0. \tag{64}$$

An implicit-explicit time integration algorithm of Hughes et al. [50, 51], was developed and implemented for use with the DRBEM. This algorithm consists of satisfying the following equations

$$M\ddot{U}_{n+1} + \Gamma^I \dot{U}_{n+1} + \Gamma^E \widetilde{\dot{U}}_{n+1} + K^I U_{n+1} + K^E \widetilde{U}_{n+1} = \mathbb{Q}_{n+1}, \tag{65}$$
$$U_{n+1} = \widetilde{U}_{n+1} + \gamma\Delta\tau^2 \ddot{U}_{n+1}, \tag{66}$$
$$\dot{U}_{n+1} = \widetilde{\dot{U}}_{n+1} + \alpha\Delta\tau \ddot{U}_{n+1}, \tag{67}$$

where

$$\widetilde{U}_{n+1} = U_{n+1} + \Delta\tau\dot{U}_n + (1-2\gamma)\frac{\Delta\tau^2}{2}\ddot{U}_n, \tag{68}$$
$$\widetilde{\dot{U}}_{n+1} = \dot{U}_n + (1-\alpha)\Delta\tau\ddot{U}_n, \tag{69}$$

In which the implicit and explicit parts are respectively denoted by the superscripts I and E. Also, we used the quantities $\widetilde{U}_{n+1}$ and $\widetilde{\dot{U}}_{n+1}$ to denote the predictor values, and U_{n+1} and $\dot{U}_{n+1}$ to denote the corrector values. It is easy to recognize that the equations (66)-(69) correspond to the Newmark formulas [52].

At each time-step, equations (65)-(69), constitute an algebraic problem in terms of the unknown $\ddot{U}_{n+1}$. The first step in the code starts by forming and factoring the effective mass

$$M^* = M + \gamma\Delta\tau C^I + \gamma\Delta\tau^2 K^I. \tag{70}$$

The time step $\Delta\tau$ must be constant to run this step. As the time-step $\Delta\tau$ is changed, the first step should be repeated at each new step. The second step is to form residual force

$$\mathbb{Q}^*_{n+1} = \mathbb{Q}_{n+1} - C^I \widetilde{\dot{U}}_{n+1} - C^E \widetilde{\dot{U}}_{n+1} - K^I \widetilde{U}_{n+1} - K^E \widetilde{U}_{n+1}. \tag{71}$$

Note that in the implicit part, M^* is always non symmetric. However, M^* still possesses the usual "band-profile" structure associated with the connectivity of the DRBEM mesh, and has a symmetric profile. So the third step is to solve $M^*\ddot{U}_{n+1} = \mathbb{Q}^*_{n+1}$ using a Crout elimination algorithm [53] which fully exploits that structure in that zeroes outside the profile are neither stored nor operated upon. The fourth step is to use predictor-corrector equations (66) and (67) to obtain the corrector displacement and velocity vectors, respectively.

The stability analysis of the algorithm under consideration has been discussed in detail in Hughes and Liu [51] and the stability conditions have also been derived in the same reference, therefore does not strictly apply to the considered problem.

4. Numerical results and discussion

The heat source is assumed to be

$$Q = Q_0\delta(x - V\tau)\delta(y)H(\tau) \tag{72}$$

where Q_0 is a prescribed value of the non-dimensional heat source, $\delta(.)$ and $H(.)$ are Dirac and Heaviside unit step function

Following Rasolofosaon and Zinszner [54] monoclinic North Sea sandstone reservoir rock was chosen as an anisotropic material and physical data are as follows:

Elasticity tensor

$$C_{abfg} = \begin{bmatrix} 17.77 & 3.78 & 3.76 & 0.24 & -0.28 & 0.03 \\ 3.78 & 19.45 & 4.13 & 0 & 0 & 1.13 \\ 3.76 & 4.13 & 21.79 & 0 & 0 & 0.38 \\ 0 & 0 & 0 & 8.30 & 0.66 & 0 \\ 0 & 0 & 0 & 0.66 & 7.62 & 0 \\ 0.03 & 1.13 & 0.38 & 0 & 0 & 7.77 \end{bmatrix} GPa \tag{73}$$

Mechanical temperature coefficient

$$\beta_{ab} = \begin{bmatrix} 0.001 & 0.02 & 0 \\ 0.02 & 0.006 & 0 \\ 0 & 0 & 0.05 \end{bmatrix} \cdot 10^6\ N/Km^2 \tag{74}$$

Tensor of thermal conductivity is

$$k_{ab} = \begin{bmatrix} 1 & 0.1 & 0.2 \\ 0.1 & 1.1 & 0.15 \\ 0.2 & 0.15 & 0.9 \end{bmatrix} W/Km \tag{75}$$

Mass density $\rho = 2216$ kg/m^3 and heat capacity $c = 0.1$ J/(kg K). The numerical values of the temperature and displacement are obtained by discretizing the boundary into 120 elements ($N_b = 120$) and choosing 60 well-spaced out collocation points ($N_i = 60$) in the interior of the solution domain, refer to the recent work of Fahmy [55].

The initial and boundary conditions considered in the calculations are

at $= 0$, $u_1 = u_2 = \dot{u}_1 = \dot{u}_2 = 0,\ T = 0$ (76)

at $x = 0$ $\quad \frac{\partial u_1}{\partial x} = \frac{\partial u_1}{\partial x} = 0, \frac{\partial T}{\partial x} = 0$ (77)

at $x = \underline{\gamma}$ $\quad \frac{\partial u_1}{\partial x} = \frac{\partial u_1}{\partial x} = 0, \frac{\partial T}{\partial x} = 0$ (78)

at $y = 0$ $\quad \frac{\partial u_1}{\partial y} = \frac{\partial u_1}{\partial y} = 0, \frac{\partial T}{\partial y} = 0$ (79)

at $y = \underline{\beta}$ $\quad \frac{\partial u_1}{\partial y} = \frac{\partial u_1}{\partial y} = 0, \frac{\partial T}{\partial y} = 0$ (80)

The present work should be applicable to coupled theories of thermoelasticity. The results are plotted in figures 2-4 for the Green and Lindsay (G-L) theory and plotted in figures 5–7 for the Lord and Shulman (L-S) theory to show the variation of the temperature T and the displacements u_1 and u_2 with x coordinate. We can conclude from these figures that the temperature T and the displacement u_1 decrease with increasing x and the displacement u_2 increases with increasing x for the two theories. It has been found that the comparison between these theories evaluates the effect of second thermal relaxation time taken by Green and Lindsay. These results obtained with the DRBEM have been compared graphically with those obtained using the finite element method (FEM) method of Xia et al. [14]. It can be seen from these figures that the DRBEM results are in excellent agreement with the results obtained by FEM, thus confirming the accuracy of the DRBEM.

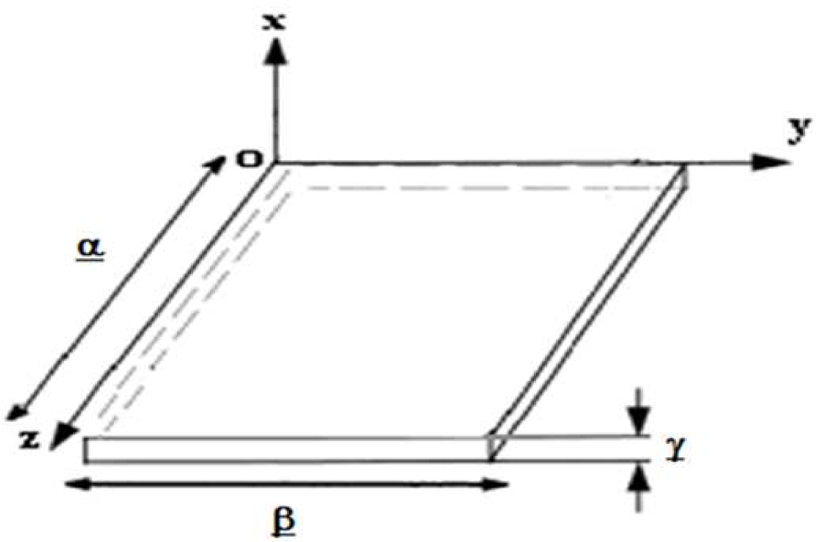

Fig. 1. The coordinate system of the FGAP.

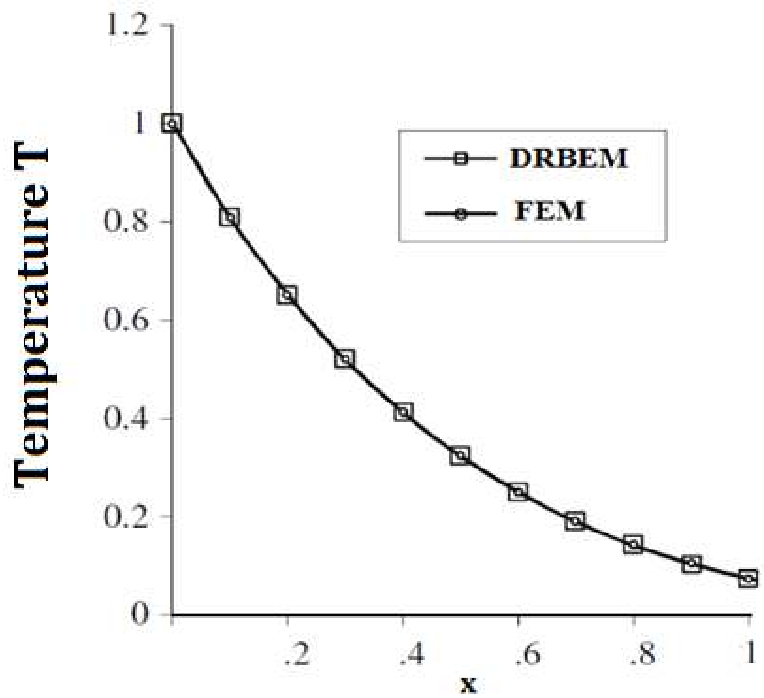

Fig. 2. Temperature distribution for G-L theory.

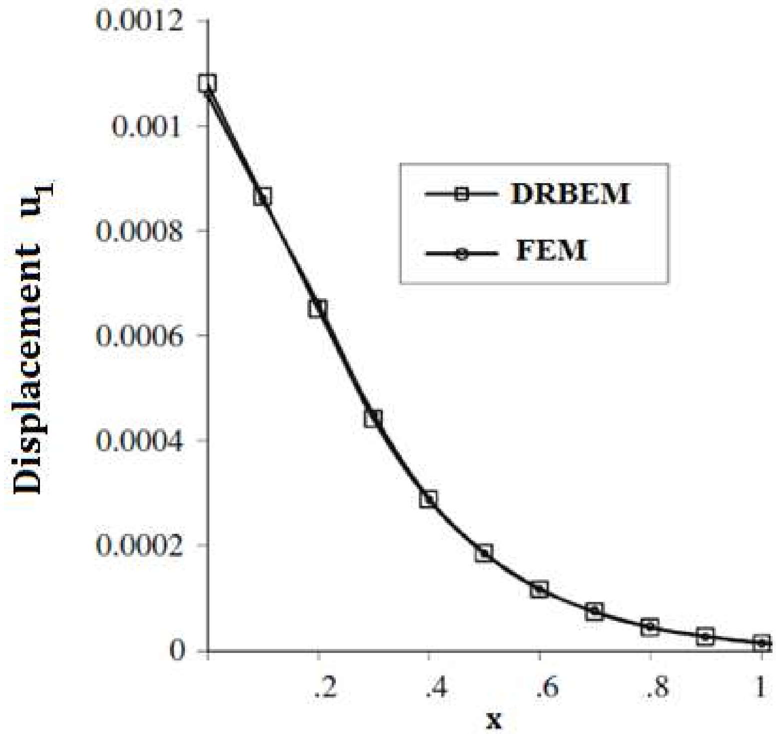

Fig. 3. Displacement distribution for G-L theory.

237

238

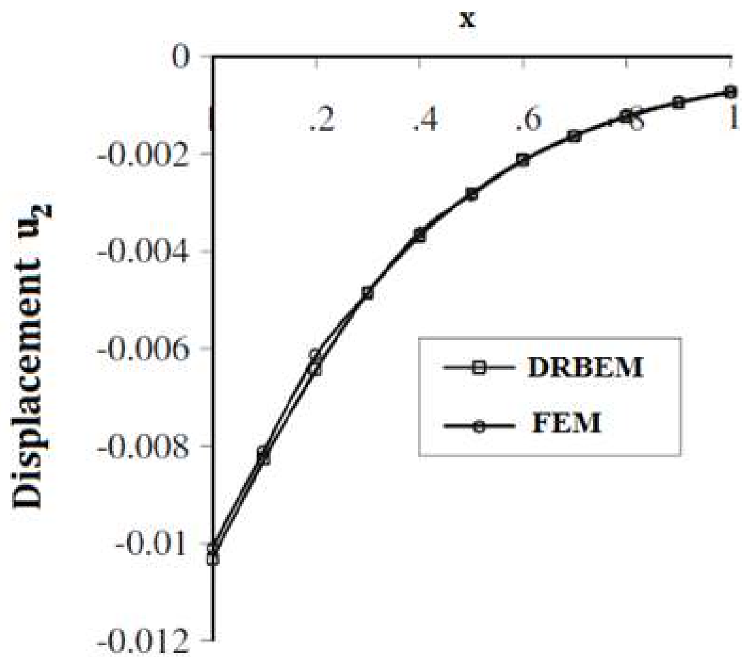

Fig. 4. Displacement distribution for G-L theory.

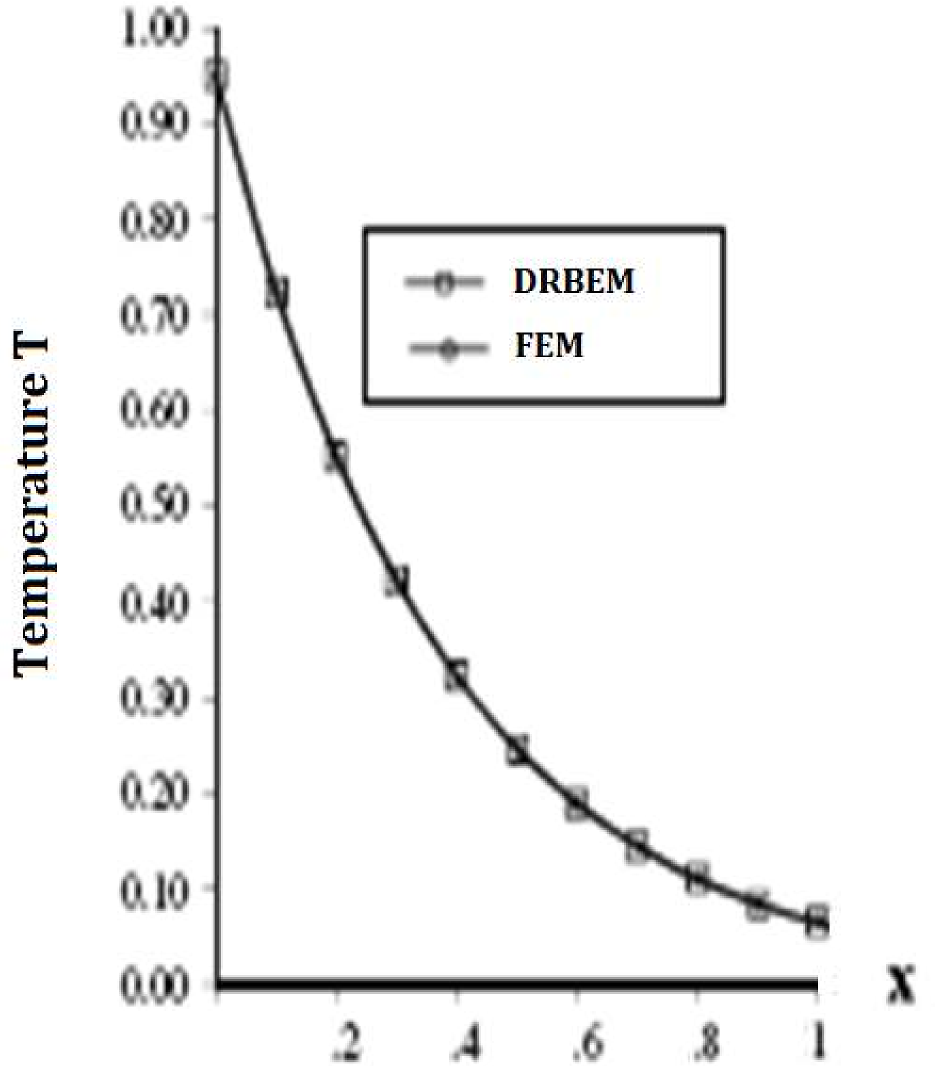

Fig. 5. Temperature distribution for L-S theory.

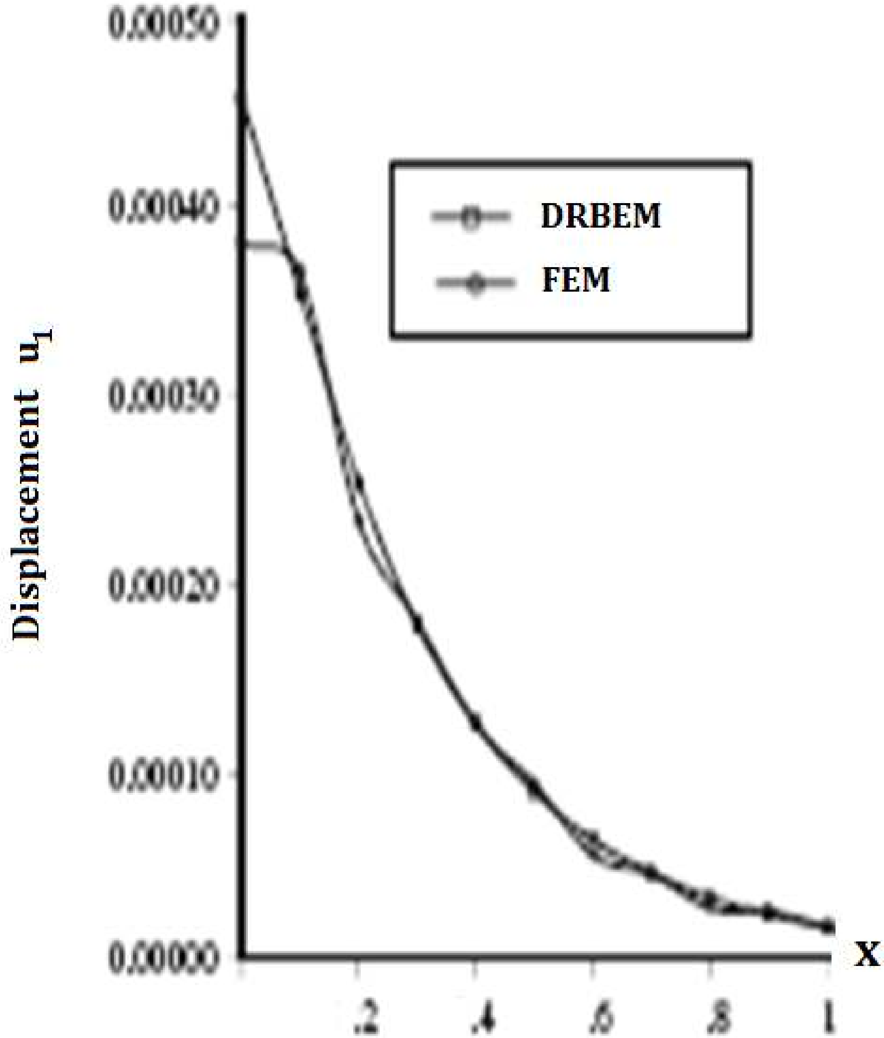

Fig. 6. Displacement distribution for L-S theory.

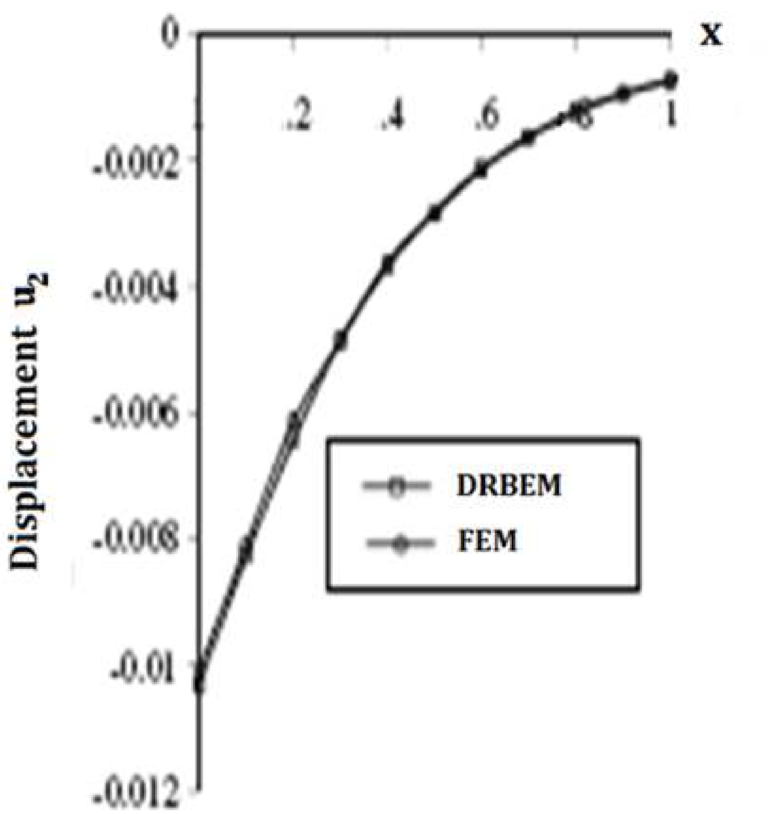

Fig. 7. Displacement distribution for L-S theory.

References

[1] Biot M. A. , Thermo-elasticity and irreversible thermodynamics, J. Appl. Phys. 27 (1956), pp.240-253.

[2] Lord H. W. and Shulman Y. A. , generalized dynamical theory of thermo-elasticity, J. Mech. Phys. Solids 15 (1967), pp. 299-309.

[3] Green A. E. and Lindsay K. A. , Thermo-elasticity J. Elast. 2 (1972), pp. 1-7.

[4] Skouras E. D., Bourantas G. C., Loukopoulos V. C., Nikiforidis G. C., Truly meshless localized type techniques for the steady-state heat conduction problems for isotropic and functionally graded materials, Eng. Anal. Boundary Elem., 35:452-464, 2011.

[5] Mojdehi A. R., Darvizeh A., Basti A., Rajabi H., Three dimensional static and dynamic analysis of thick functionally graded plates by the meshless local Petrov-Galerkin (MLPG) method, Eng. Anal. Boundary Elem, 35:1168-1180, 2011.

[6] Zhou F. X., Li S. R. and Lai Y. M. Three-Dimensional Analysis for Transient Coupled Thermoelastic Response of a Functionally Graded Rectangular Plate, J. of Sound and Vibration, vol. 330, pp. 3990–4001, 2011.

[7] Loghman A, Aleayoub S. M. A, Sadi M. H., Time-dependent magnetothermoelastic creep modeling of FGM spheres using method of successive elastic solution, Appl. Math. Modell, 36:836-845, 2012.

[8] Sun D. and Luo S. N. Wave Propagation and Transient Response of a Functionally Graded Material Plate under a Point Impact Load in Thermal Environments, Appl. Mathematical Modelling, vol. 36, pp. 444–462, 2012.

[9] Mirzaei D., Dehghan M., New implementation of MLBIE method for heat conduction analysis in functionally graded materials, Eng. Anal. Boundary Elem., 36:511-519, 2012.

[10] Abd-Alla, A. N., Relaxation effects on reflection of generalized magneto-thermo-elastic waves, Mechanics Research Communications, 27:591–600, 2000.

[11] Abd-Alla, A. N. and Al-Dawy, A. A. S., Thermal relaxation times effect on Rayleigh waves in generalized thermoelastic media, Journal of Thermal Stresses, 24:367-382, 2001.

[12] Abbas, I. A. and Abd-Alla, A. N., A study of generalized thermoelastic interaction in an infinite fibre-reinforced anisotropic plate containing a circular hole, Acta Physica Polonica A, 119:814-818, 2011a.

[13] Abbas, I. A., Abd-Alla, A. N., Effect of initial stress on a fiber-reinforced anisotropic thermoelastic thick plate, International Journal of Thermophysics, 32:1098-1110, 2011b.

[14] Xia R., Tian X. and Shen Y., Dynamic response of two-dimensional generalized thermoelastic coupling problem subjected to a moving heat source, Acta Mechanica Solida Sinica, 27:300-305, 2014.

[15] El-Naggar A. M., Abd-Alla A. M., Fahmy M. A., Ahmed S. M., Thermal stresses in a rotating non-homogeneous orthotropic hollow cylinder, Heat Mass Transfer, 39:41-46, 2002.

[16] El-Naggar A. M., Abd-Alla A. M., Fahmy M. A., The propagation of thermal stresses in an infinite elastic slab, Appl. Math. Comput, 157:307-312, 2004.

[17] Abd-Alla A. M., El-Naggar A. M., Fahmy M. A., Magneto-thermoelastic problem in non-homogeneous isotropic cylinder, Heat Mass Transfer, 39:625-629, 2003.

[18] Abd-Alla A. M, Fahmy M. A, El-Shahat T. M., Magneto-thermo-elastic stresses in inhomogeneous anisotropic solid in the presence of body force, Far East J. Appl. Math., 27:499-516, 2007.

[19] Abd-Alla A. M, Fahmy M. A, El-Shahat T. M., Magneto-thermo-elastic problem of a rotating non-homogeneous anisotropic solid cylinder, Arch. Appl. Mech., 78:135-148, 2008.

[20] Qin Q. H., 2D Green's functions of defective magnetoelectroelastic solids under thermal loading, Eng. Anal. Boundary Elem., 29:577-585, 2005.

[21] Sladek V., Sladek J., Tanaka M., Zhang Ch., Local integral equation method for potential problems in functionally graded anisotropic materials, Eng. Anal. Boundary Elem., 29:829-843, 2005.

[22] Tian X, Shen Y, Chen C and He T., A direct finite element method study of generalized thermoelastic problems, International Journal of Solids and Structures, 43:2050-2063, 2006.

[23] Fahmy M. A., Effect of initial stress and inhomogeneity on magneto-thermo-elastic stresses in a rotating anisotropic solid, JP J. Heat Mass Transfer., 1:93-112, 2007.

[24] Fahmy M. A., Thermoelastic stresses in a rotating non-homogeneous anisotropic body,“ Numer. Heat Transfer, Part A., 53:1001-1011, 2008.

[25] Fahmy M. A., Thermal stresses in a spherical shell under three thermoelastic models using FDM, Int. J. Numer. Methods Appl., 2:123-128, 2009.

[26] Fahmy M. A., Finite difference algorithm for transient magneto-thermo-elastic stresses in a non-homogeneous solid cylinder. Int. J. Mater. Eng. Technol., 3:87-93, 2010a.

[27] Fahmy M. A., Influence of inhomogeneity and initial stress on the transient magneto-thermo-visco-elastic stress waves in an anisotropic solid, World J. Mech., 1:256-265, 2011b.
[28] Fahmy M. A., Numerical modeling of transient magneto-thermo-viscoelastic waves in a rotating nonhomogeneous anisotropic solid under initial stress, Int. J. Model. Simul. Sci. Comput., 3, 125002, 2012b.
[29] Fahmy M. A., El-Shahat T. M., The effect of initial stress and inhomogeneity on the thermoelastic stresses in a rotating anisotropic solid," Arch. Appl. Mech., 78:431-442, 2008.
[30] Othman M. I. A., Song Y., Effect of rotation on plane waves of generalized electro-magneto-thermoviscoelasticity with two relaxation times, Appl. Math. Modell., 32:811–825, 2008.
[31] Davì G., Milazzo A., A regular variational boundary model for free vibrations of magneto-electro-elastic structures, Eng. Anal. Boundary Elem., 35:303-312, 2011.
[32] Hou P. F., He S., Chen C. P., 2D general solution and fundamental solution for orthotropic thermoelastic materials, Eng. Anal. Boundary Elem., 35:56-60, 2011.
[33] Abreu A. I., Canelas A., Sensale B., Mansur W. J. [2012] "CQM-based BEM formulation for uncoupled transient quasistatic thermoelasticity analysis," Eng. Anal. Boundary Elem., 36:568-578, 2012.
[34] Espinosa J. V., Mediavilla A. F., Boundary element method applied to three dimensional thermoelastic contact, Eng. Anal. Boundary Elem., 36:928-933, 2012.
[35] Nardini D., Brebbia C. A., A new approach to free vibration analysis using boundary elements, in: C. A. Brebbia (Eds.), Boundary elements in engineering, Springer, Berlin, 312-326, 1982.
[36] Brebbia C. A., Telles J. C. F., Wrobel L. Boundary element techniques in Engineering, (Springer-Verlag, New York), 1984.
[37] Wrobel L. C., Brebbia C. A., The dual reciprocity boundary element formulation for nonlinear diffusion problems, Comput. Methods Appl. Mech. Eng., 65:147-164, 1987.
[38] Partridge P. W., Brebbia C. A., Computer implementation of the BEM dual reciprocity method for the solution of general field equations, Commun. Appl. Numer. Methods, 6:83-92, 1990.
[39] Partridge P. W., Wrobel L. C., The dual reciprocity boundary element method for spontaneous ignition. Int. J. Numer. Methods Eng., 30:953–963, 1990.
[40] Fahmy M. A., Application of DRBEM to non-steady state heat conduction in non-homogeneous anisotropic media under various boundary elements, Far East J. Math. Sci., 43:83-93, 2010b.
[41] Fahmy M. A., A time-stepping DRBEM for magneto-thermo-viscoelastic interactions in a rotating nonhomogeneous anisotropic solid," Int. J. Appl. Mech, 3:1-24, 2011a.
[42] Fahmy M. A., A time-stepping DRBEM for the transient magneto-thermo-visco-elastic stresses in a rotating non-homogeneous anisotropic solid, Eng. Anal. Boundary Elem., 36:335-345, 2012a.
[43] Fahmy M. A., Transient magneto-thermo-elastic stresses in an anisotropic viscoelastic solid with and without moving heat source, Numer. Heat Transfer, Part A., 61:547-564, 2012c.
[44] Fahmy M. A., Transient magneto-thermoviscoelastic plane waves in a non-homogeneous anisotropic thick strip subjected to a moving heat source, Appl. Math. Modell, 36:4565-4578, 2012d.
[45] Fahmy M. A., Transient magneto-thermo-viscoelastic stresses in a rotating nonhomogeneous anisotropic solid with and without a moving heat source, J. Eng. Phys. Thermophys, 85:874-880, 2012e.
[46] Fahmy, M. A., The DRBEM solution of the generalized magneto-thermo-viscoelastic problems in 3D anisotropic functionally graded solids, Proceeding of V International conference on coupled problems in science and engineering, Ibiza, Spain, pp. 862-872, 2013.
[47] Fahmy, M. A., Boundary Element Solution of 2D Coupled Problem in Anisotropic Piezoelectric FGM Plates, Proceedings of the VI International Conference on Computational Methods for Coupled Problems in Science and Engineering, Venice. Italy. pp. 382-391, 2015.

[48] Partridge P. W., Brebbia C. A., Wrobel L. C., The dual reciprocity boundary element method, (Computational Mechanics Publications, Boston, Southampton), 1992.
[49] Gaul L., Kögl M. and Wagner M., Boundary element methods for engineers and scientists, (Springer-Verlag, Berlin), 2003.
[50] Hughes T. J. R. and Liu W. K., Implicit-Explicit finite element in Transient analysis: Stability theory,“ ASME J. Appl. Mech., 45:371-374, 1978a.
[51] Hughes T. J. R. and Liu W. K., Implicit-Explicit finite element in Transient analysis: Implementation and numerical examples, “ ASME J. Appl. Mech., 45:375-378, 1978b.
[52] Newmark N. M., A method of computation for structural dynamics, J. Eng. Mech. Div., 85:67-94, 1959.
[53] Taylor R. L., Computer procedures for finite element analysis,“ in: O.C. Zienckiewicz (Third Edition), The finite element method, (McGraw Hill, London), 1977.

[54] Rasolofosaon P. N. J., Zinszner B. E., Comparison between permeability anisotropy and elasticity anisotropy of reservoir rocks, Geophys., 67:230-240, 2002.
[55] Fahmy M. A., Implicit–Explicit Time Integration DRBEM for Generalized Magneto-Thermoelasticity Problems of Rotating Anisotropic Viscoelastic Functionally Graded Solids., Engineering Analysis with Boundary Elements. 37:107-115, 2013.